AIAA JOURNAL
Vol. 31, No. 12, December 1993

Numerical Simulations of Flutter and its Suppression by Active Control

J. Alan Luton* and Dean T. Mook†
Virginia Polytechnic Institute and State University, Blacksburg, Virginia 24061

A method for predicting the unsteady, subsonic, aeroservoelastic response of a wing has been developed. The air, wing, control surface, and control system are considered to be elements of a single dynamical system. All equations are solved simultaneously in the time domain by an iterative scheme based on a predictor-corrector method. The scheme allows a wide range of nonlinear aerodynamic and structural models to be used and subcritical, critical, and supercritical aeroelastic behavior can be modeled without restrictions to small disturbances or periodic motions. In this paper, a general unsteady vortex-lattice method is used to model the aerodynamics. This method accounts for nonlinear effects associated with high angles of attack, unsteady behavior, large deformations of the wing, and the convection of vorticity. Two structural models have been employed: a linear model and a nonlinear model that accounts for finite curvature. Both models consider the flexural-torsional motion of an inextensional wing. A feedback-control system that governs the motion of control surfaces is implemented to suppress the motion of the wing. Results show that the suppression of flutter by means of active control is readily possible at velocities well beyond the flutter speed and that limit cycle solutions might exist near the flutter speed.

Nomenclature

$B_m(t)$ = natural coordinates of flexure
$C_m(t)$ = natural coordinates of torsion
dt = dimensionless time step
EI = flexural stiffness
G_1, G_2, G_3, G_4 = gains of the control laws
GJ = torsional stiffness
g = acceleration of gravity
J_0 = mass polar moment of inertia
L = dimensionless semispan, nondimensionalized by L_c
L_c = characteristic length, 0.2 m
M = number of torsional modes
m = mass per unit span
N = number of flexural modes
$Q_b(t)$ = dimensionless aerodynamic force per unit span
$Q_t(t)$ = dimensionless aerodynamic twisting moment per unit span
t = dimensionless time, t^*V/L_c
t_i = dimensionless time at time step i
$u(y,t)$ = spanwise displacement of the wing, nondimensionalized by L_c
V = freestream velocity
$v(y,t)$ = lateral displacement of the wing, nondimensionalized by L_c
y = spanwise coordinate, nondimensionalized by L_c
α = angle of attack of the undeformed wing
ΔC_m = change in C_m from the static solution
δ = aileron rotation
δ_c = aileron command rotation
ζ = aileron viscous damping ratio
ρ = freestream air density
$\phi(y,t)$ = twist of the wing
$\chi_m(y)$ = linear, undamped, natural modes for torsion
$\psi_m(y)$ = linear, undamped, natural modes for flexure
$\omega_{b,i}$ = undamped natural frequency of the ith mode of flexure
ω_n = undamped natural frequency of the aileron, nondimensionalized by V/L_c
$\omega_{t,i}$ = undamped natural frequency of the ith mode of torsion

Superscripts

* = physical quantity
$\dot{()}$ = derivative with respect to t
$()'$ = derivative with respect to y

Subscripts

LE = leading edge
TE = trailing edge

Presented as Paper 92-4652 at the AIAA Atmospheric Flight Mechanics Meeting, Hilton Head, SC, Aug. 10-12, 1992; received Jan. 9, 1993; revision received May 26, 1993; accepted for publication May 26, 1993.

*Graduate Research Assistant, Engineering Science and Mechanics Department.
†N. Waldo Harrison Professor, Engineering Science and Mechanics Department. Member AIAA.

Introduction

THERE is currently a desire to develop high-altitude, long-endurance (HALE) aircraft capable of obtaining air samples at altitudes difficult to reach by balloon (see, for instance, Ref. 1). Studies of the ozone layer require data at altitudes of 100,000 ft and higher. Designs of such aircraft feature lightweight, high-aspect-ratio wings that are very flexible. Active control could be an important mechanism in ensuring the dynamic stability of these wings.

Research on active flutter suppression has been pursued for many years. Edwards et al.,[2] Horikawa and Dowell,[3] Karpel,[4] and Batina and Yang[5] are a few who have studied the active flutter control of airfoils. Many different methods have been used to design control systems for flutter suppression. Classical feedback control techniques are often used, and the energy concept of Nissim[6-8] has also been shown to be effective. One difficulty in finding an optimal control law is the approximation of the unsteady aerodynamic forces in the state space. Rational approximations for the aerodynamic forces for arbitrary motions of a lifting surface have been developed by several researchers.[9-12] Padé approximants[2,5] and the minimum state method[4,13] have been widely used to approximate

the aerodynamic forces. With the addition of the structural equations and a control law, a control analysis may be performed. The current approach integrates the equations of motion in the time domain, which eliminates the approximation of the aerodynamic forces but prevents the use of optimal control theory.

Time-marching integration schemes based on CFD methods have been used to investigate flutter in the transonic regime. This regime is important since the flutter speed is typically lowest here. The main emphasis has been on the accurate modeling of the unsteady aerodynamic forces. The transonic potential equation has been applied to the flutter of airfoils[14,15] and wings.[16,17] More recently, the Euler equations have been used.[18,19] Different integration schemes have been employed. Borland and Rizzetta[20] and Guruswamy[18] used centered-difference techniques whereas Edwards et al.[15] and Rausch et al.[19] used predictor-corrector schemes.

The current study, however, is focused on very flexible wings operating in the subsonic regime. Motions of the wing are not necessarily small or harmonic. It builds on the work of Konstadinopoulos et al.,[21] who modeled wing rock of delta wings; Mracek and Mook,[22] who investigated the use of control systems to suppress wing rock; Dong,[23] who used feedback control to suppress the flutter of an airfoil; and Strganac and Mook,[24] who used a procedure similar to the present one, but without a control system. The wing and surrounding air are treated as a single dynamical system, and the equations of motion for the wing and the fluid are solved simultaneously in the time domain. The coupled differential equations are solved by an iterative scheme based on the Hamming predictor-corrector numerical-integration algorithm.[25,26] The elastic wing is modeled as an inextensional cantilevered beam (i.e., one whose length does not change) that experiences flexural-torsional motions. In addition, a nonlinear formulation of an inextensional wing that accounts for finite curvature is also used. The loads are provided by a general unsteady vortex-lattice method and nonlinearities due to angle of attack and static or dynamic deformations are included. The geometry of the wake and the distribution of vorticity in the wake are also part of the solution. The vorticity currently in the wake was shed from the wing at an earlier time so the history of the motion is stored in the wake.

The control system consists of leading-edge and trailing-edge ailerons near the wing tips that are moved in accordance with various control laws. These control laws are based on data that could be obtained from accelerometers placed near the wing tips. A servolaw that models the servomotor is also used. The response of the wing to initial disturbances is examined with and without active control in the subcritical and supercritical flutter regimes at subsonic Mach numbers.

The approach is modular, so different aerodynamic and structural models as well as different control laws and servo-equations can be inserted to replace those used in the present examples without changing the basic algorithm.

Aerodynamic Model

The general unsteady vortex-lattice method used in this paper is a fully three-dimensional model that can simulate arbitrary subsonic maneuvers of wings of arbitrary planform at arbitrary angles of attack as long as stall and/or vortex bursting do not occur. Aerodynamic nonlinearities due to large angles of attack and deformations of the wing are included as well. The ability of this method to accurately predict the static loads has been demonstrated.[27]

The general unsteady vortex-lattice method was described previously by Konstadinopoulos et al.[27] and is only briefly reviewed here. The wing is modeled as a vortex sheet bound to the camber surface of the wing. The vortex sheet is approximated by a finite number of vortex filaments that form a grid (known as the bound lattice). The grid is composed of closed loops of constant-circulation, straight, vortex filaments in order to satisfy the requirement of spatial conservation of vorticity. The circulation around a vortex filament that is part of two loops is the difference between the loop circulations of the adjoining panels. The values of the loop circulations are found by simultaneously imposing the no-penetration condition on the wing at the control points of the panels. The control point is the centroid of the corners of the panel. The velocity at a point is the sum of the contributions from every vortex filament in the bound lattice and free lattice (the wake) as calculated by the Biot-Savart law. The unsteady Kutta condition requires that the vortex segments along the edges that adjoin the wake be shed. This shed vorticity forms the wake and is convected at the local particle velocity in accord with the Kelvin-Helmholtz theorem. This is realized by convecting the end points of the vortex segments in the wake. Thus, a force-free wake (i.e., no pressure discontinuities) is created, which contains the vorticity shed from the wing. The position of the wake and the distribution of vorticity within it are part of the solution. The wake, therefore, contains information from the past which affects the wing at the present; it is the "historian" of the flow. When a vortex segment is convected far enough downstream that it no longer influences the flow near the wing, it is neglected. Since the unsteady vortex-lattice method can model arbitrary wing geometries and motions, a control system can easily be incorporated into the model. The aileron rotations are specified by the control laws. The known positions and velocities of the control points of the aileron panels allows the aerodynamic equations to be solved and the unsteady forces on the ailerons to be found. A flowfield predicted by the vortex-lattice method is depicted in Fig. 1. The complementary semispan not shown is symmetric.

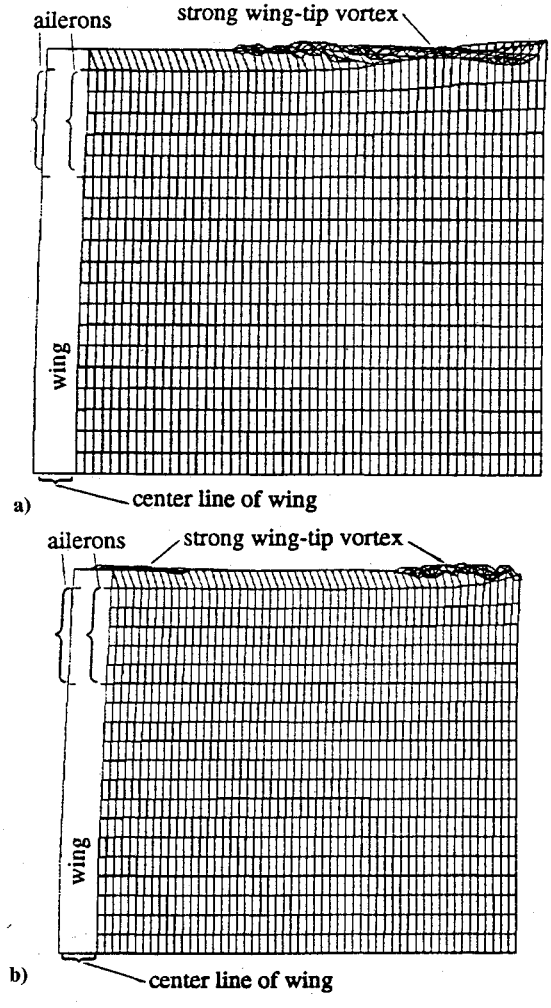

Fig. 1 Two top views of the wing and the lattice representing the wake at different times during the upward motion of the wing tip: a) upward motion of the wing is large and the wing-tip vortex being generated is weak and b) wing is stopping and a strong wing-tip vortex is starting to form.

To make Fig. 1, we first imagined the wing to be fixed in its undeformed position and then calculated the corresponding steady flowfield. The relatively high loads generated a strong wing-tip vortex. Next we released the wing, and as the wing tip accelerated upward, the wing-tip vortex was weakened. In Fig. 1a, one sees a top view of the wing as the wing tip accelerates upward. The remnants of the strong wing-tip vortex can still be seen about halfway down the wake. In Fig. 1b, one sees a strong wing-tip vortex system reforming; the wing tip is now decelerating as it nears its maximum upward deflection. The remnants of the original strong wing-tip vortex can be seen much farther downstream.

Although these strong vortex systems do not dominate the flowfield, they do significantly contribute to the torque and force near the wing tip, which for a very flexible wing means that they also significantly contribute to the deflections.

The aerodynamic loads on the wing are calculated from the pressure jumps at the control points of the panels of the bound lattice. The pressure jump is found by using the unsteady Bernoulli equation.

Structural Model

The solution scheme for the aeroservoelastic problem does not in any way limit the choice of a structural model for the wing. The numerical integration scheme is capable of handling any nonlinearities associated with the aerodynamics, inertia, material, geometry, and control system. Two different structural models of the wing are examined: a nonlinear model that accounts for finite curvature and its linearized form. The nonlinear model is not meant for a comprehensive study of nonlinear effects but for a demonstration of the ability of the present formulation to model structural nonlinearities. A complete nonlinear model should include extensional effects and coupling between bending and torsion. Both formulations model the wing as an inextensional cantilevered beam that can bend and twist as shown in Fig. 2. To emphasize the aerodynamic coupling between torsion and flexure, the inertial axis is aligned with the elastic axis. Also, material properties are assumed to be constant along the span. Neither assumption is necessary.

The governing equations for the motion of the wing were developed by Luton[26] and are given (in dimensionless form) by

$$\ddot{\phi} - D_t\phi'' = q_t Q_t \tag{1a}$$

$$\ddot{v} + D_b v'''' - D_b(2v'^2 v'''' + 10v'v''v''' + 3v''^3) = q_b Q_b - W - \tfrac{1}{2} q_b Q_b v'^2 \tag{1b}$$

$$u(y,t) = -\frac{1}{2}\int_0^y v'^2\, dy \tag{1c}$$

where

$$D_b = \frac{EI}{mL_c^2 V^2}, \quad D_t = \frac{GJ}{V^2 J_0}, \quad q_b = \frac{\rho L_c^2}{2m}, \quad q_t = \frac{\rho L_c}{2J_0}, \quad W = \frac{gL_c}{V^2}$$

The equations have been nondimensionalized by the characteristic variables V, L_c, and ρ. The boundary conditions are

$$\begin{aligned} \phi(0,t) &= 0 & \phi'(L,t) &= 0 \\ v(0,t) &= 0 & v''(L,t) &= 0 \\ v'(0,t) &= 0 & v'''(L,t) &= 0 \end{aligned} \tag{2}$$

For the nonlinear model, the displacement in the y direction, u, can be found after the lateral displacement has been found. The nonlinear terms of Eq. (1b) are due to curvature effects. For the linear equations these terms are zero and $u(y,t) = 0$. Although the flexural and torsional motions are structurally uncoupled, they are coupled through the aerodynamic loads. The loads depend on the shape and motion of the wing at the current time and at previous times

$$Q_t = Q_t(v, \dot{v}, \phi, \dot{\phi}, \text{ and their histories}) \tag{3a}$$

$$Q_b = Q_b(v, \dot{v}, \phi, \dot{\phi}, \text{ and their histories}) \tag{3b}$$

The procedure is to solve Eqs. (1) and those governing the flow for u, v, ϕ, Q_t, and Q_b simultaneously.

The lateral displacement and angle of twist are represented by expansions in terms of the linear, undamped, natural modes, or

$$\phi(y,t) = \sum_{m=1}^{M} C_m(t)\chi_m(y) \tag{4a}$$

$$v(y,t) = \sum_{m=1}^{N} B_m(t)\psi_m(y) \tag{4b}$$

In this study, four flexural modes and three torsional modes were used. The mode shapes satisfy the boundary conditions and can be obtained by any means. In the current work they have been derived analytically, but they could have been found by using a detailed finite element model. The expansions are substituted into the governing equations, Eqs. (1), and Galerkin's procedure is applied to produce a set of $N + M$ second-order ordinary differential equations, as shown in Ref. 26, which govern the natural coordinates $C_m(t)$ and $B_m(t)$. The equations are then written as a set of $2(N + M)$ first-order equations for the numerical integration scheme.

Control System

The aeroelastic response of a wing can be modified in such a way as to increase stability and performance while minimizing weight. The methods of controlling the aeroelastic responses fall into two broad categories: passive and active. Passive methods include changing the shape or mass distribution of a lifting surface, changing the stiffness, and/or reducing the flight speed. Active methods involve moving control surfaces according to control laws based on output from sensors placed in the wing. In the current work, for flutter suppression, the control system uses ailerons that are moved as flaps, and the control laws have the form

$$\delta_{c,\mathrm{TE}}(t) = G_1\dot{v}(0.95L,t) + G_2\dot{\phi}(0.95L,t) \tag{5a}$$

$$\delta_{c,\mathrm{LE}}(t) = G_3\dot{v}(0.95L,t) + G_4\dot{\phi}(0.95L,t) \tag{5b}$$

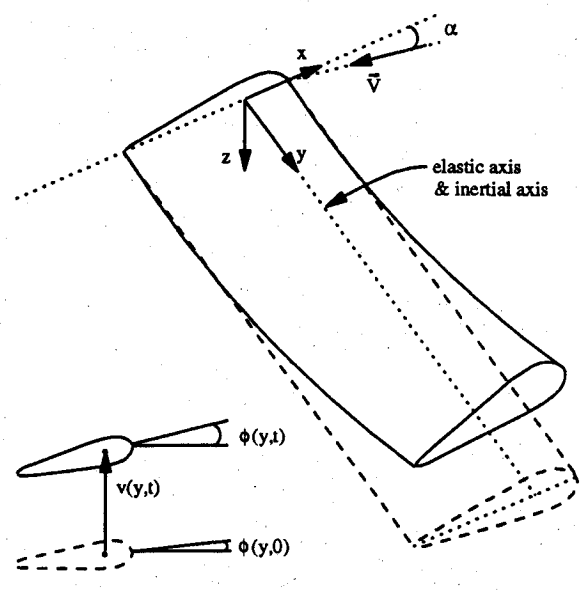

Fig. 2 Torsional and flexural degrees of freedom of the wing.

In the examples presented subsequently the gains were selected by a trial-and-error procedure. The sensors are assumed to supply $\dot{v}$ and $\dot{\phi}$ at the spanwise location of $y/L = 0.95$. The actual aileron deflections are found from the commanded deflections by the use of a servolaw which is intended to model the characteristics of the servomotor. The servolaw used here is

$$\ddot{\delta} + 2\zeta\omega_n\dot{\delta} + \omega_n^2\delta = \omega_n^2\delta_c \tag{6}$$

The ailerons were limited to ± 12-deg rotations and zero angular velocity at these extreme positions. The choice of control laws and servolaws is not limited to linear equations or constant gains.

Numerical Integration Schemes

In the present paper both static and dynamic solutions have been found. The static solution is useful as an initial condition for the dynamic analysis. The static solution is obtained by iteration. First steady torsional and flexural deformations are assumed (usually zero). Then the steady aerodynamic loads are computed. These loads are then used to compute a new steady deformation. The process is repeated until convergence or aeroelastic divergence occurs.

The algorithm for the dynamic solution is based on Hamming's fourth-order predictor-corrector method[25] and is depicted in Fig. 3. A multistep method was chosen rather than a one-step method (such as Runge-Kutta) because it is best to calculate the aerodynamic loads only at integral time steps. The predictor-corrector method requires the state variables (the natural coordinates and their time derivatives) and the aerodynamic loads at the current time step and the three previous time steps. The solution at the first three time steps is obtained by a special starting procedure (see Ref. 26). After the first three time steps, advancing the solution one time step from $t = t_i$ to t_{i+1} involves convecting the wake to its new position, moving the ailerons according to Eqs. (5) and (6), and applying the predictor-corrector integrator. The state variables at $t = t_{i+1}$ are first predicted and then used with the vortex-lattice method to predict the loads on the wing at $t = t_{i+1}$. Next the loads are used to improve (i.e., "correct") the prediction of the state of the wing, and then the resulting state is used to recorrect the loads. This process is repeated until convergence. Final corrections to the state and loads are made and the complete solution at $t = t_{i+1}$ is then known. Typically two or three iterations are required at each time step.

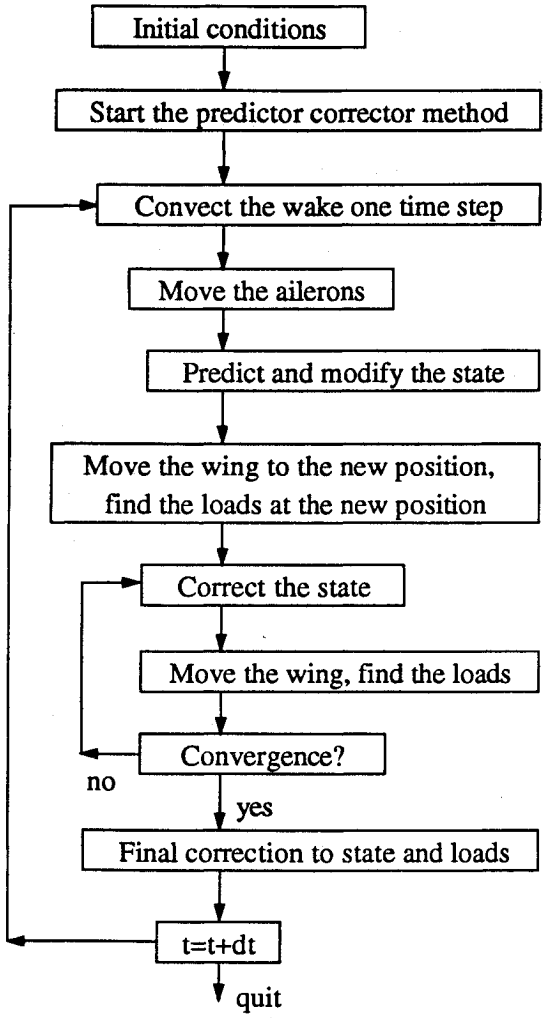

Fig. 3 Algorithm for the dynamic solution.

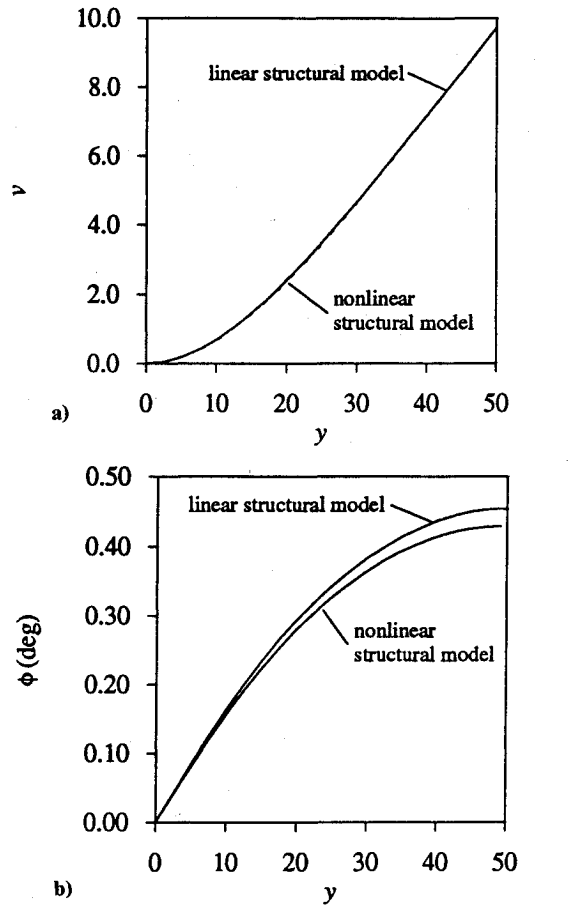

Fig. 4 Comparison of the static deformations obtained from the linear and nonlinear structural models: a) lateral displacement and b) twist angle of the wing.

Table 1 Physical properties of the wing and air used in the examples

Chord, m	1.0
Aspect ratio	20.0
Elastic axis, m	0.305 from leading edge
Inertial axis, m	0.305 from leading edge
m, kg/m	10.0
J_0, kg-m	15.0
GJ, N-m^2	0.2493×10^6
EI, N-m^2	0.3686×10^6
ζ	0.5
ω_n^*, rad/s	393
ρ^*, kg/m^3	1.0572
Undamped natural frequencies, Hz	
$\omega_{b,1} = 1.07$	$\omega_{t,1} = 3.22$
$\omega_{b,2} = 6.73$	$\omega_{t,2} = 9.63$
$\omega_{b,3} = 18.85$	$\omega_{t,3} = 16.11$
$\omega_{b,4} = 61.07$	

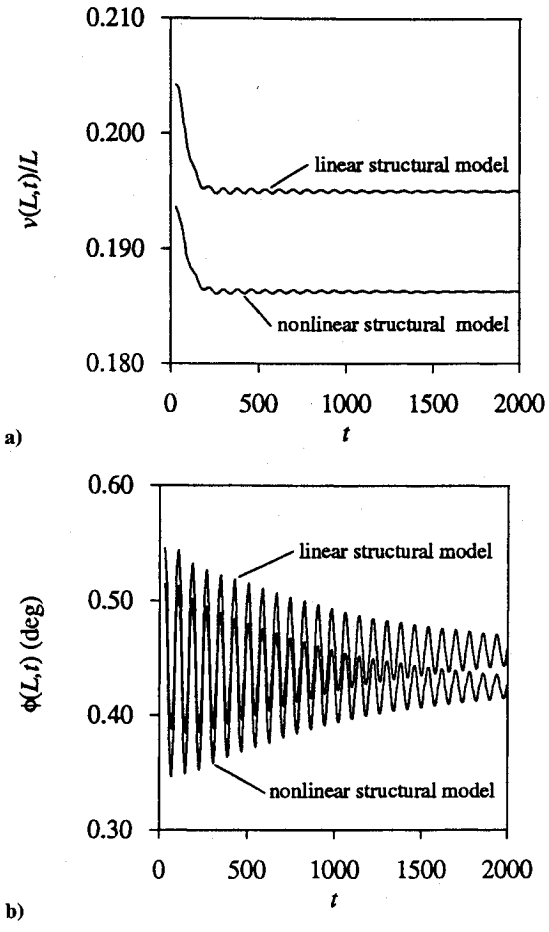

Fig. 5 Subcritical response of the wing tip to an initial disturbance with the linear and nonlinear structural models: a) wing-tip deflection and b) wing-tip rotation as functions of time.

The dimensionless time step is chosen to make the size of the elements in the wake approximately the same as those on the wing.

Examples

The procedure is demonstrated by examples that include simulations both below and above the critical flutter speed. Although the method allows spanwise variation of structural properties, a wing with constant properties has been selected. The properties of the wing and air used in all of the examples are given in Table 1. In the following examples, the freestream velocity is increased while the angle of attack is decreased to keep the lift approximately constant.

The static solutions for the linear and nonlinear structural models are shown in Fig. 4 as the lateral displacement v and twist ϕ along the elastic axis for $V = 50$ m/s and $\alpha = 5.9$ deg. The curvature terms appear to have a negligible effect. The solutions for v are nearly coincident although the twist of the wing has changed slightly despite the fact that the twist and bending are not coupled in the structural equations. This change in twist is due to the aerodynamic coupling between the bending and torsion loads. Because $u(y) < 0$ the curve for the nonlinear structural model stops short of $y = 50$.

In Fig. 5 the dynamic response of the wing is shown when a slight initial disturbance is given to each of the natural coordinates from their static values of Fig. 4. Again, solutions employing the linear and nonlinear structural models are shown. The lateral deflection and twist at the wing tip are plotted as functions of dimensionless time. The flexural motion is highly damped and the torsional oscillations decay with a frequency near the first-mode natural frequency (reduced frequency = 0.0129). The oscillations for both solutions are about mean values equal to those found by the static solution. It is emphasized that all of the damping is due to the aerodynamic loads (there is no structural damping in the present model). These loads are predicted by what is often called an inviscid theory; thus, there is inviscid damping as a result of the transfer of energy from the structure to the flowing air.

Three different solutions near the flutter speed are shown in Figs. 6–8. At speeds slightly below the flutter speed the disturbance decays very slowly, as shown in Fig. 6. The speed is 75 m/s and $\alpha = 2.4$ deg. At $V = 80$ m/s (see Fig. 8) the disturbance grows quite slowly. The twist response is similar to the flexure response in both instances. However, the solution for $V = 77.5$ m/s, shown in Fig. 7, is locked into a stable oscillatory motion of constant amplitude. This suggests that there

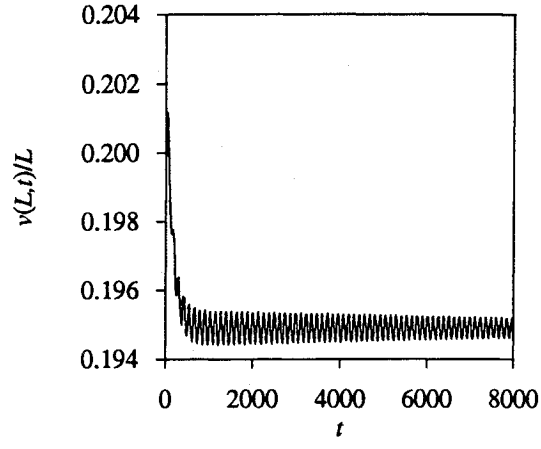

Fig. 6 Slightly subcritical response to an initial disturbance: wing-tip deflection as a function of time.

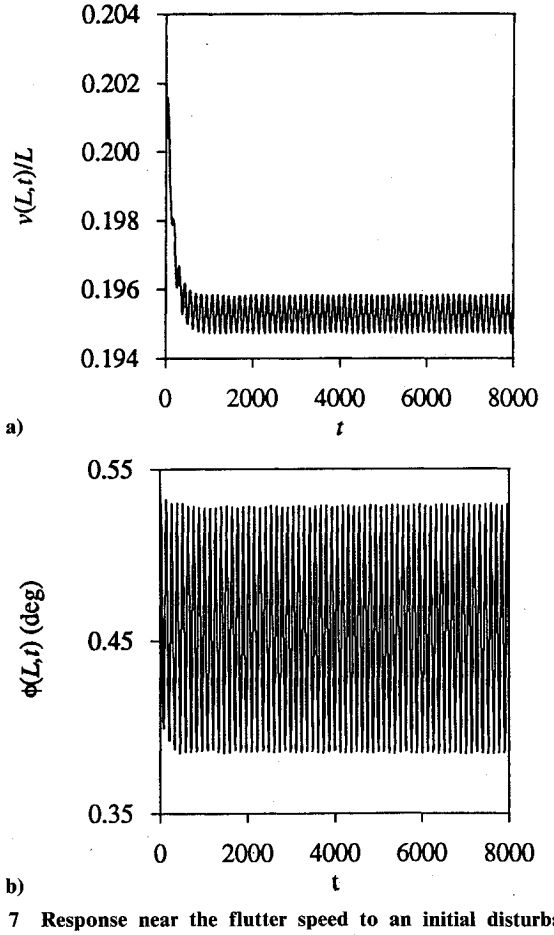

Fig. 7 Response near the flutter speed to an initial disturbance, showing the development of a limit cycle: a) wing-tip deflection and b) wing-tip rotation as functions of time.

are limit-cycle solutions in the neighborhood of the flutter speed. Dong[23] found such limit-cycle solutions, whose amplitudes were proportional to the velocity, for a rigid airfoil mounted on an elastic support. The linear structural model has been used in the solution, so all nonlinearities come from the aerodynamics.

A supercritical response of the wing, where $V = 125$ m/s and $\alpha = 0.65$ deg, is shown in Fig. 9. The oscillations appear to grow exponentially with a common frequency near the first torsional natural frequency (reduced frequency = 0.0052). The nonlinear structural model is again used in the solution. In Fig. 10 the same supercritical response is shown when the control system is turned on at $t = 2000$. The gains are $G_1 = -5$, $G_2 = 500$, $G_3 = 0$, and $G_4 = 0$ (only the trailing-edge

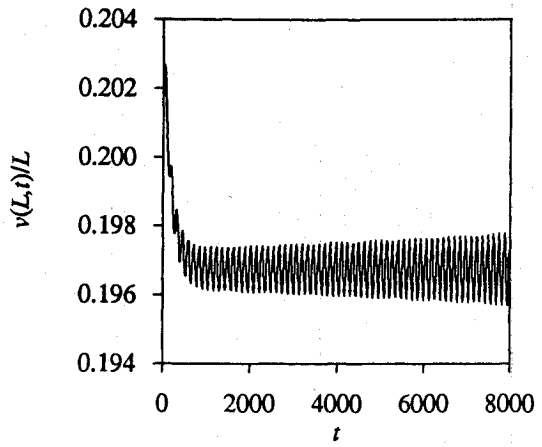

Fig. 8 Slightly supercritical response to an initial disturbance: wing-tip deflection as a function of time.

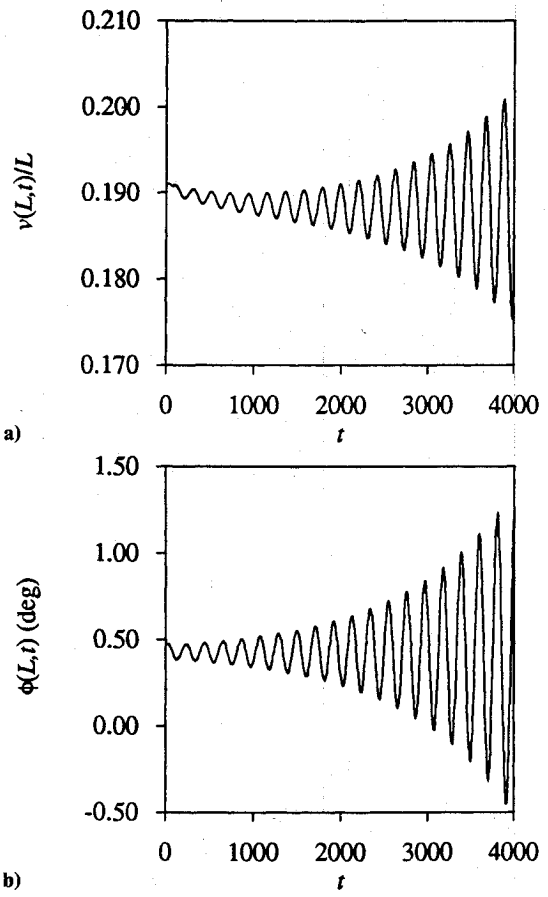

Fig. 9 Strongly supercritical response to an initial disturbance: a) wing-tip deflection and b) wing-tip rotation as functions of time.

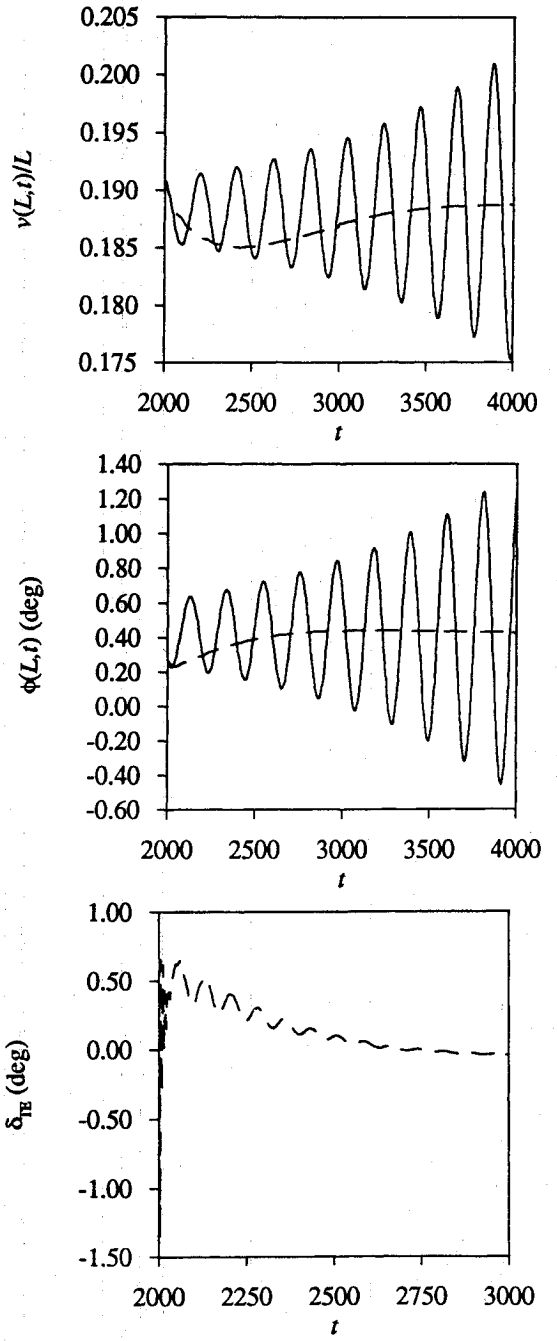

Fig. 10 Response of the wing with (dashed line) and without (solid line) control: a) wing-tip deflection, b) wing-tip rotation, and c) aileron rotation as functions of time.

ailerons are activated). Despite the fact that the oscillations have already progressed to moderate values, the actively controlled aileron is able to stabilize the system very quickly. The trailing-edge aileron deflections are shown in Fig. 10c. The deflections are quite reasonable. If there is no delay in activating the control system, then the deflections are much smaller. In fact, when the control system was activated without delay, flutter was suppressed at a speed of 150 m/s (see Ref. 26). Although the flap deflections appear to decay to zero, small oscillations are always needed to maintain stability. If the control system is turned off, then small disturbances quickly grow. If both trailing-edge and leading-edge ailerons are activated then the response is similar, but a steady state can be reached somewhat faster.

One concern associated with the use of active control is that oscillations of the control surface might excite one of the high-frequency modes of the wing. Then energy from the

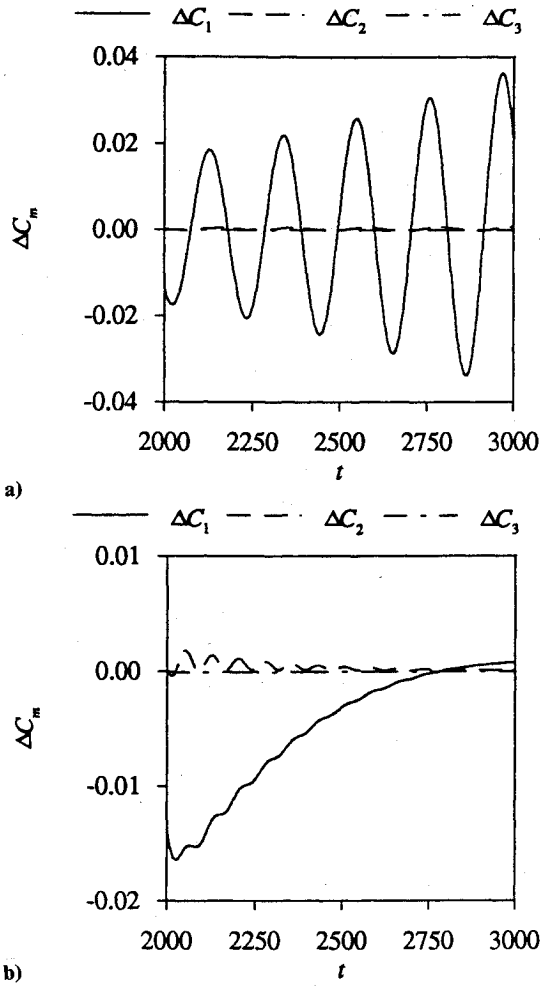

Fig. 11 Change in the torsional natural coordinates from their static solutions: a) control system deactivated and b) control system activated.

low-amplitude, high-frequency mode might be passed via a nonlinear mechanism, such as an internal or autoparametric resonance, to a high-amplitude, low-frequency mode (see, e.g., Haddow et al.[28] and Nayfeh and Balachandran[29]) with the result of dangerously large oscillations and structural damage. The effect of the control system on the natural coordinates is shown in Fig. 11. The deviations of the torsional natural coordinates from the static solution are plotted as a function of dimensionless time. Figure 11a shows the response without the control system while Fig. 11b shows the response with the control system activated. Initially the second mode of torsion is significantly excited by the control system, but it decays as the amplitude of the aileron deflections decays. In this case the excited second mode of torsion does not destroy the stability of the system. The first two torsional modes and the aileron deflection (after transients decay) all oscillate with a common frequency significantly higher than the flutter frequency.

Concluding Remarks

A general formulation for simulating aeroservoelastic behavior has been presented. The general formulation is modular, and, consequently, different methods for solving for the flowfield and different structural models can be used without changing the basic algorithm. Aerodynamic, material, inertial, and geometric nonlinear effects may be included. Motions in the subcritical, critical, and supercritical regimes can be simulated with no prior assumptions as to the form of the solution (e.g., periodic motions). The present approach is applicable to subsonic flows over very flexible wings. In such situations, large deflections are expected. Applications could include some sailplanes and high-altitude, long-endurance (HALE) aircraft.

In this paper, a general unsteady vortex-lattice method is used to find the aerodynamic loads. This model is valid in the subsonic regime as long as separation and/or vortex bursting do not occur. The vortex-lattice method is capable of accurately determining the unsteady loads and the position of the wake.[27] Nonlinear effects due to angle of attack, static deformations, and dynamic deformations are also included.

Two structural models have been used in the aeroelastic formulation: a linear model and a nonlinear model that accounts for large curvature. In both cases the wing is modeled as an inextensional cantilevered beam that experiences flexural-torsional motion. Simulations have shown that static solutions obtained by using the two different models agree closely for bending deflections at the wing tip up to 20% of the semispan; thus, the nonlinear effects of curvature appear to be negligible in the simulations examined in this work. However, a complete nonlinear study that includes flexural-torsional coupling and extensional effects should be performed to gain more conclusive information about the relative importance of the nonlinearities. The current work is intended to demonstrate the ability to include structural nonlinearities.

A relatively simple, linear feedback control system has been successfully used to suppress flutter in the present simulation. The control system consists of one or more ailerons whose motion is based on the velocity of the wing tip ($\dot{v}$ and $\dot{\phi}$) and corresponding constant gains as well as a servolaw representing the servomotor. The present simulation is also capable of incorporating nonlinear control laws and variable gains. The gains for the current study were selected by a trial-and-error procedure. It was found that a wide range of gains is effective in the suppression of flutter. The control system can suppress flutter at almost twice the flutter speed. Much higher flutter speeds might be obtained by selecting an appropriate control law and optimal gains. Although no attempt has been made to find the power requirements necessary for the aileron motion, it appears that only very small deflections and low frequencies are needed, especially when there is little or no delay in activating the control system.

Acknowledgment

This work was supported by the Air Force Office of Scientific Research under Contract AFOSR-90-0032.

References

[1]Henderson, B. W., "Boeing Condor Raises UAV Performance Levels," *Aviation Week and Space Technology*, April 23, 1990, pp. 36–38.

[2]Edwards, J. W., Breakwell, J. V., and Bryson, A. E., Jr., "Active Flutter Control Using Generalized Unsteady Aerodynamic Theory," *Journal of Guidance and Control*, Vol. 1, No. 1, 1978, pp. 32–40.

[3]Horikawa, H., and Dowell, E. H., "An Elementary Explanation of the Flutter Mechanism with Active Feedback Control," *Journal of Aircraft*, Vol. 16, No. 4, 1979, pp. 225–232.

[4]Karpel, M., "Design for Active Flutter Suppression and Gust Alleviation Using State-Space Aeroelastic Modeling," *Journal of Aircraft*, Vol. 19, No. 3, 1982, pp. 221–227.

[5]Batina, J. T., and Yang, T. Y., "Application of Transonic Codes to Aeroelastic Modeling of Airfoils Including Active Controls," *Journal of Aircraft*, Vol. 21, No. 8, 1984, pp. 623–630.

[6]Nissim, E., "Flutter Suppression Using Active Controls Based on the Concept of Aerodynamic Energy," NASA TN D-6199, March 1971.

[7]Nissim, E., "Comparative Study Between Two Different Active Flutter Suppression Systems," *Journal of Aircraft*, Vol. 15, No. 12, 1978, pp. 843–848.

[8]Nissim, E., "Active Controls for Flutter Suppression and Gust Alleviation in Supersonic Aircraft," *Journal of Guidance and Control*, Vol. 3, No. 4, 1980, pp. 345–351.

[9]Vepa, R., "Finite-State Modeling of Aeroelastic Systems," NASA CR-2779, Feb. 1977.

[10]Roger, K. L., "Airplane Math Modeling Methods for Active Control Design," AGARD-CP-228, Aug. 1977, pp. 4-1–4-11.

[11]Mahesh, J. K., Stone, C. R., Garrand, W. L., and Dunn, H. J.,

"Control Law Synthesis for Flutter Suppression Using Linear Quadratic Gaussian Theory," *Journal of Guidance and Control*, Vol. 4, No. 4, 1981, pp. 415–422.

[12]Mukhopadhyay, V., Newsom, J. R., and Abel, I., "Reduced-Order Optimal Feedback Control Law Synthesis for Flutter Suppression," *Journal of Guidance and Control*, Vol. 5, No. 4, 1982, pp. 389–395.

[13]Noll, T. E., "Aeroservoelasticity," NASA TM 102620, March 1990.

[14]Rizzetta, D. P., "Time-Dependent Response of a Two-Dimensional Airfoil in Transonic Flow," *AIAA Journal*, Vol. 17, No. 1, 1979, pp. 26–32.

[15]Edwards, J. W., Bennett, R. M., Whitlow, W., Jr., and Seidel, D. A., "Time-Marching Transonic Flutter Solutions Including Angle-of-Attack Effects," *Journal of Aircraft*, Vol. 20, No. 11, 1983, pp. 899–906.

[16]Eastep, F. E., and Olsen, J. J., "Transonic Flutter Analysis of a Rectangular Wing with Conventional Airfoil Sections," *AIAA Journal*, Vol. 18, No. 10, 1980, pp. 1159–1164.

[17]Cunningham, H. F., Batina, J. T., and Bennett, R. M., "Modern Wing Flutter Analysis by Computational Fluid Dynamics Methods," *Journal of Aircraft*, Vol. 25, No. 10, 1988, pp. 962–968.

[18]Guruswamy, G. P., "Unsteady Aerodynamic and Aeroelastic Calculations for Wings Using Euler Equations," *AIAA Journal*, Vol. 28, No. 3, 1990, pp. 461–469.

[19]Rausch, R. D., Batina, J. T., and Yang, H. T. Y., "Euler Flutter Analysis of Airfoils Using Unstructured Dynamic Meshes," *Journal of Aircraft*, Vol. 27, No. 5, 1990, pp. 436–443.

[20]Borland, C. J., and Rizzetta, D. P., "Nonlinear Transonic Flutter Analysis," *AIAA Journal*, Vol. 20, No. 11, 1982, pp. 1606–1615.

[21]Konstadinopoulos, P., Mook, D. T., and Nayfeh, A. H., "Subsonic Wing Rock of Slender Delta Wings," *Journal of Aircraft*, Vol. 22, No. 3, 1985, pp. 223–228.

[22]Mracek, C. P., and Mook, D. T., "Aerodynamic Potential Flow Panel Method Coupled with Dynamics and Controls," AIAA Atmospheric Flight Mechanics Conference, AIAA Paper 91-2846, New Orleans, LA, Aug. 1991.

[23]Dong, B., "Numerical Simulations of Wakes, Blade-Vortex Interaction, Flutter, and Flutter Suppression by Feedback Control," Ph.D. Dissertation, Dept. of Engineering Science and Mechanics, Virginia Polytechnic Inst. and State Univ., Blacksburg, VA, Aug. 1991.

[24]Strganac, T. W., and Mook, D. T., "Numerical Model of Unsteady Subsonic Aeroelastic Behavior," *AIAA Journal*, Vol. 28, No. 5, 1990, pp. 903–908.

[25]Carnahan, B., Luther, H. A., and Wilkes, J. O., *Applied Numerical Methods*, Wiley, New York, 1969.

[26]Luton, J. A., "Numerical Simulations of Subsonic Aeroelastic Behavior and Flutter Suppression by Active Control," M.S. Thesis, Dept. of Engineering Science and Mechanics, Virginia Polytechnic Inst. and State Univ., Blacksburg, VA, Dec. 1991.

[27]Konstadinopoulos, P., Thrasher, D. F., Mook, D. T., Nayfeh, A. H., and Watson, L., "A Vortex-Lattice Method for General, Unsteady Aerodynamics," *Journal of Aircraft*, Vol. 22, No. 1, 1985, pp. 43–49.

[28]Haddow, A. G., Barr, A. D. S., and Mook, D. T., "Theoretical and Experimental Study of Modal Interaction in a Two-Degree-of-Freedom Structure," *Journal of Sound and Vibration*, Vol. 97, Dec. 1984, pp. 451–473.

[29]Nayfeh, A. H., and Balachandran, B., "Modal Interactions in Dynamical and Structural Systems," *Applied Mechanics Reviews*, Vol. 42, Nov. 1989, pp. 175–201.